Indian Journal of Science and Technology, Vol 8(28), DOI: 10.17485/ijst/2015/v8i28/87172, October 2015
ISSN (Print) : 0974-6846
ISSN (Online) : 0974-5645

Investigating Behavior of Cantilever Beams of Normal and Lightweight Reinforced Concrete under Cyclic Load

Farrokh Agamohammadzadeh[1], Hassan Afshin[2*] and Masoud Nekoei[1]

[1]Department of Civil Engineering, Science and Research Branch, Islamic Azad University,Tehran, Iran; Farrokh.am@gmail.com, MsNekooei@gmail.com

[2]Civil Engineering Faculty, Sahand University of Technology, Sahand, Iran; HassanAfshin@yahoo.com

Abstract

Background/Objectives: Investigation the behavior of lightweight aggregate concrete beams and connection under cyclic loading and compare it with the behavior of concrete beam with normal weight. **Methods/Statistical Analysis:** This study is focused on the experimental investigation of the behavior of the beams constructed of scoria lightweight aggregate concrete. Five samples of cantilever beams are developed; tree of which are made of lightweight aggregate concrete, while two are made of normal weight concrete. In this paper, performance of the plastic hinge in the flexural beams made of lightweight aggregate concrete is investigated based on the stiffness reduction parameters, pinching phenomena, strength reduction, and ductility. **Findings:** The results showed that beam stiffness, independent from strength, is reduced with increase in the displacement cycles and in the high deformation cycles, pinching phenomenon occurs randomly. Also, strength is not reduced with increase in amplitude of the cycles until reaching displacement ductility 4 and flexural behaviors of normal and reinforced lightweight aggregate concretes are the same value. In deformation cycles with the amplitude of 80mm, equivalent to ductility 4, no significance decrease in the strength is observed in force–deformation curve. With respect to ratio of the shear span to significant depth of the test specimens, the flexural behavior is dominant and the beams endure ductility of greater than 4. It is concluded that the reinforced lightweight aggregate concrete beams with maximum lightweight aggregate size of smaller than 5mm have ductility behavior during the bending, similar to the reinforced normal concrete beams. **Application/Improvements:** The results demonstrated that in flexural beams, type of concrete (lightweight or normal aggregate) does not have particular influence on the stiffness reduction.

Keywords: Cantilever Beam, Cyclic Loading, Ductility, Hysteretic Diagram, Lightweight Concrete, Stiffness Deterioration

1. Introduction

In seismic areas, the force caused by earthquake has a considerable effect on the structures and the main force on structures is caused by the force of earthquake. Considering the fact that each structure is affected by force of earthquake in proportion to its weight, one method to reduce force of earthquake is reduction in dead load of buildings. Since size of structural elements is relatively large in reinforced concrete structures, reducing specific weight of the concrete can significantly reduce the structure's dead load. By employing different types of lightweight aggregate materials and providing appropriate mix design, it is possible to manufacture lightweight concrete with sufficient strength. This type of concrete not only provides the advantage of having a low weight material, but also has acceptable level of strength and durability equal to the normal weight concrete. Reducing the dead load will result in decreased force of earthquake, size of beams, columns, and foundation, minimum required rebar, and costs. It could also increase the required space via reducing size of columns, slabs,

* Author for correspondence

and beams. Due to insulation, lightweight concrete prevents thermal energy loss and provides relatively good resistance to fire.

In normal weight concrete, because of higher strength of aggregate than the concrete mortar, the failure surface passes around the aggregates and, as a result, the failure surface would be a ridged and rough surface which prevents the two surfaces around the shear cracks from slipping over each other; even after the shear crack, resistance would be generated due to the friction between these rough surfaces, which prevents the sudden shear degradation of the element[1]. However, due to the lower strength of the lightweight aggregate than that of the mortar, in the lightweight aggregate concrete, the failure surface passes through the lightweight aggregate and, as a result, after the concrete is cracked, both sides of the failure surface would be flat; this issue would cause the two flat surfaces to slip on each other without any resistance in the diagonal cracks caused by shear failure which lack resistance to degradation. According to the above-mentioned discussion, it is concluded that the elements made of lightweight aggregate concrete are brittle and have less ductility than those constructed of normal weight concrete.

Structures should have the ductility necessary for bearing force of earthquake. Considering the fact that, in structures, beam failure mechanisms provide more ductility than the column failure mechanisms and the impact of beam ductility is more significant than that of columns. Also, according to the fact that, in most of the lightweight concrete structures, floors and beams are made of lightweight concrete and columns are made of normal weight concrete, it is necessary to examine ductility of the beams made of the lightweight aggregate concrete.

In elements of ductile reinforced concrete, after the elements are yielded, plastic deformation would be concentrated in a small area of element length which is called plastic hinge. Performance of plastic hinge determines the behavior of elements based on load capacity and deformation[2]. In most ductile beams; plastic hinge is formed on the side of the column at the beam-column connection. Formation of the plastic hinge on the side of the column is a result of yielding longitudinal rebar in this area[3].

In previous years, some investigations have been conducted on the behavior of beam-column sub-assemblage under loading similar to earthquake[4–7]. The aim of the present study is to investigate the behavior of plastic hinge at the end of a beam made of natural lightweight aggregate concrete under cyclic loading and to compare it with the behavior of beam constructed of normal weight concrete. To accomplish this goal, the element connected to the column is tested such that the column acts as a horizontal support for the vertical beam element. In other words, the beam is located as a vertical element under flexural and shearing effects. Horizontal deformation at the free end of each specimen is applied to the beam with no external axial force. Horizontal deformation is applied to the beam so as to obtain its behavior in the elastic and inelastic regions.

2. Experimental Procedure

To investigate the behavior of the beam and connection under cyclic loading, five elements of reinforced beam-column sub-assemblage with the scale of 1:2 were prepared from a building frame according to Figure 1 for the tests. Size of the sample cross-sections was 20cm × 20cm and length of the beam was 150cm. The main re-bars included 4 re-bars with the diameter of 12mm and the shear re-bar was a rebar with the diameter of 8mm and interval of 10cm (Figure 1). Three specimens were made of lightweight aggregate concrete, while two remaining were made of concrete with normal weight. The scoria aggregate with the maximum grain size of 5mm was used to prepare concrete; also, cylinder strength of lightweight aggregate concrete and its specific weight were obtained respectively as 27MPa and 1800kgf/m^3. The normal weight concrete was prepared as a mixture of natural aggregate with the grade of 300kg cement per m^3, which presented the strength of 21MPa.

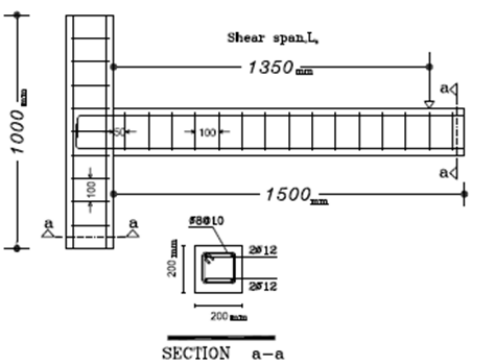

Figure 1. Scheme of the tested specimen.

Using the test results, shear force-displacement curve was plotted for the free end of the beam and the overall performance of the structure was investigated.

As shown in Figure 1, the action point of the force was at 135cm distance from the column. As a result, length of the shear span was 135cm and ratio of shear span length to depth of the beam was 6.75. To transmit the force to the beam, a sheet with the thickness of 2cm was used at the end of beam and a hinge was used at the force point of action. The column was connected to the rigid floor with bolts as a support and force was applied to the specimens using a jack that was connected to a load cell (Figure 2).

Figure 2. Connection of jack to the beam.

3. Selecting the Applied Displacement

The real effect of earthquake in nature is dynamic; but, the hysteretic test simulated in this study had a semi-static effect. However, the difference between shape of the hysteresis loops obtained from the semi-static test and dynamic test was not significant. To create a performance criterion for a ductile reinforced concrete element, it is required for the element to experience at least four full cycles of displacement history with displacement amplitude in any direction corresponding to a displacement ductility of 4[8]. In such a scenario, it is better to apply a gradual increasing cycle to the specimen in elastic and inelastic modes. Hysteresis results in the cumulative ductility equal to 32 could produce the same results. A cumulative displacement ductility of 10 has been recommended as a lower bound for a satisfactory behavior under moderate or severe earthquake loadings[5]. Displacement scenario used in this study is shown in Figure 3, in which each displacement amplitude was repeated for 3 times and the displacement amplitudes of the cycles were gradually increased in elastic and inelastic modes to the cumulative ductility of greater than 32. Therefore, it was expected that the present displacement scenario would test the specimen behavior under the semi-seismic loading with severe cracking and failure.

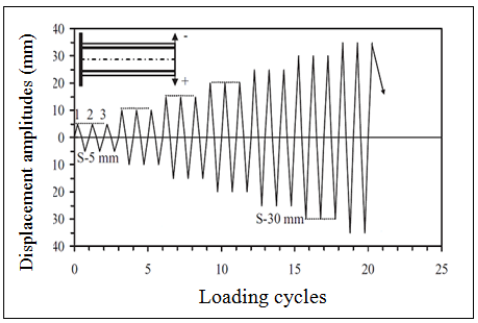

Figure 3. Displacement scheme applied for beams.

4. Hysteresis Analysis

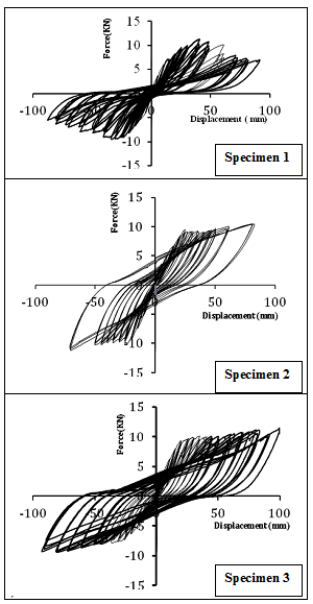

Figure 4. Hysteretic diagrams for lightweight aggregate beams.

Hysteresis behavior is expressed by equations of shear force against horizontal displacement. Hysteretic diagrams for the specimens made of lightweight concrete and normal weight concretes is shown in Figures 4 and 5, respectively. Hysteresis analysis investigates the parameters that affect

the overall form of the load-deformation equations including stiffness degradation, pinching phenomenon, and strength reduction.

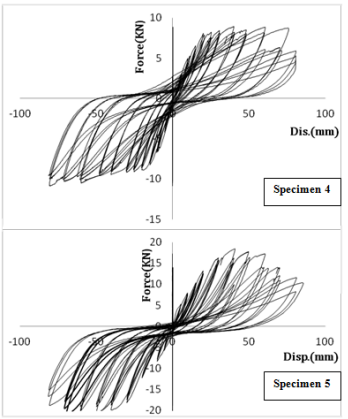

Figure 5. Hysteretic diagrams for normal weight aggregate beams.

4.1 Stiffness Degradation

At the beginning of testing each specimen, a loading is applied which ranges from 0 to the maximum loading. Then, the loading process is continued by unloading-reloading mode. In this study, different types of stiffness were investigated which included: secant stiffness k, unloading stiffness $\boldsymbol{k_{un}}$ and reloading stiffness $\boldsymbol{k_r}$ (Figure 6). Stiffness was scaled with respect to the secant stiffness at the beginning of yielding, while its variations with ductility were investigated. First, stiffness was independently obtained for each loading direction and then its average value was determined.

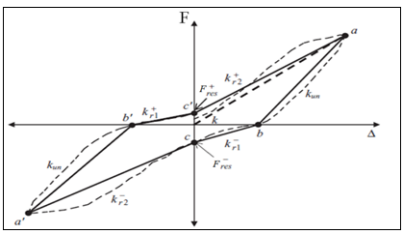

Figure 6. Designation used for stiffness types.

4.2 Secant Stiffness

Stiffness degradation indicates the secant stiffness variations during loading cycles based on the deformation applied to the element. As can be seen in Figure 6, for each loop, the secant stiffness was defined as the ratio of maximum load to the corresponding displacement. Stiffness degradation for the specimens made of lightweight concrete and normal weight concretes is shown in Figures 7 and 8, respectively. As can be seen in these figures, stiffness degradation was highly correlated with the applied displacement ductility. Displacement ductility μ has been defined as the ratio of maximum displacement Δ divided by the yield displacement Δ_y. In order to find the best relationship between them, regression analysis was conducted and Equations 1 and 2 were obtained for the element of lightweight concrete and normal weight concrete, respectively.

$$\frac{k}{k_y} = 0.951 - 0.513Ln(\mu) \quad (1)$$

$$\frac{k}{k_y} = 0.967 - 0.48Ln(\mu) \quad (2)$$

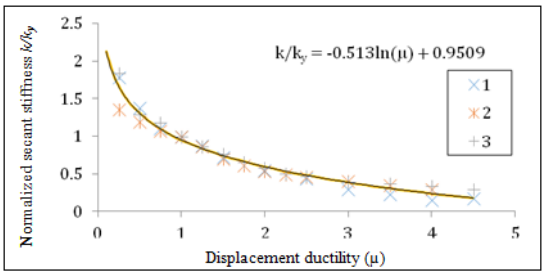

Figure 7. Variation of secant stiffness with the imposed displacement ductility for lightweight concrete.

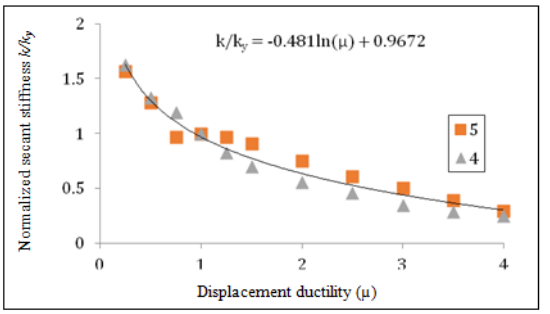

Figure 8. Variation of secant stiffness with the imposed displacement ductility for normal weight concrete.

4.3 Unloading Stiffness

In each loop, after the maximum load, tangent stiffness is reduced with decreasing load (unloading) and stiffness is minimized when the load reached zero. This issue happens because, at the points of maximum load in the loop, the cracks have their maximum value in the tensile region and start to close after unloading. During inelastic cycles, the cracks could not completely close at zero-load points due to the effect of residual tensile *strain in the re-bar*, softening of the concrete stress, and the residual

slip between re-bar and concrete, which causes residual displacement. Tangent stiffness during unloading depends on the level of displacement and the corresponding load[9]. In addition, tangent stiffness during unloading is declined with an increase in the deformation at the beginning of unloading[10]. In this study, decreased stiffness during unloading was examined using equations between hysteresis curve and the corresponding displacement ductility. For a half loading cycle (e.g. positive half), the stiffness unloading was obtained as follows:

$$k_{un} = \frac{F_i^+}{\delta_i^+ - \delta_{res}^+} \quad (3)$$

Where F_i and δ_i are respectively the load and displacement at point i and δ_{res} is residual displacement of the loop .Unloading stiffness variations have been extensively studied based on the applied ductility in the previous articles and some equations have been presented as a decreasing function as follows:

$$\frac{k_{un}}{k_y} = m\left(\frac{\delta}{\delta_y}\right)^{-n} \quad (4)$$

In these equations, k_y and δ_y are respectively the stiffness and displacement at the beginning of yielding. These equations have been used in a general form for all the hysteresis models proposed in the past[10–13]. According to the present experimental work, the unloading stiffness of the lightweight and normal weight reinforced concrete beams is shown in Figures 9 and 10. Using regression analysis, Equations 5 and 6 are recommended for lightweight and normal weight concrete, respectively.

$$\frac{k_{un}}{k_y} = 1.0866\mu^{-0.433} \quad (5)$$

$$\frac{k_{un}}{k_y} = 1.226\mu^{-0.3383} \quad (6)$$

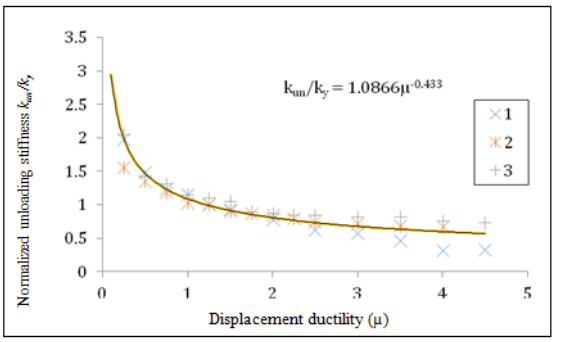

Figure 9. Variation of unloading stiffness with the imposed displacement ductility for lightweight concrete.

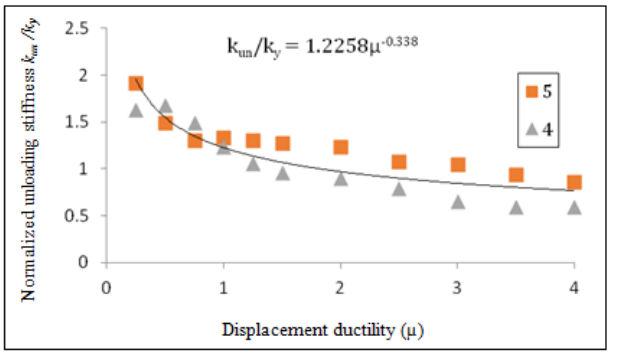

Figure 10. Figure 10. Variation of unloading stiffness with the imposed displacement ductility for normal weight concrete.

4.4 Reloading Stiffness

As mentioned earlier, at the end of unloading, there is a considerable decline in the tangent stiffness. By starting the reloading, new cracks appear again and expand on the new tensile side, while the previous cracks are not completely closed due to the residual strain and longitudinal re-bar slip. In this case, shear stresses and shear deformations have a significant impact on tangent stiffness. When the cracks are closed, there is a complete contact of the concrete surface that significantly increases the tangent stiffness at points c and c' in Figure 4[10,14]. Cracks are closed when compressive re-bar is yielded under the pressure; but, its contribution to increasing the element stiffness is possible to be reduced due to decreased stiffness of the yielded re-bar. Since the re-bar behavior is dominant in the under-reinforced beams, increase in the tangent stiffness due to the complete contact of crack surface under the yielding of the compressive re-bar might not be more important than the re-bar contribution itself. From point c' to the completion of half of the reverse cycle, the tangent stiffness is increased due to the increase in bond-slip and flexural strength caused by closure of the cracks appearing in the previous tensile area. Since loading branch causes the re-bars of tensile direction to become inelasticity, stiffness softening is not symmetrical for the two directions. Because it is difficult to show the gradual tangent stiffness, a linear change is used to show the reloading stiffness. Bilinear models have been widely accepted by researchers. The first stiffness in the reloading after completion of the unloading is shown by k_{r1}^-, while the second change is shown by k_{r2}^- that is greater than k_{r1}^-.

4.5 Reloading Stiffness k_{r1}

For a hysteresis loop, stiffness reloading k_{r1} represents the secant stiffness before the cracks are closed during half of the loading cycle. As shown in Figure 4, k_{r1} can be determined as follows:

$$k_{r1}^{-} = \frac{F_{res}^{-}}{\delta_{res}^{+}} \tag{7}$$

This stiffness is obtained from the hysteresis curves separately for each direction and then the results are averaged and scaled as $\frac{k_{r1}}{k_y}$ and are shown in Figures 11 and 12, respectively, for elements of lightweight and normal concrete. As can be seen in the figures, Equations 8 and 9 are obtained for the lightweight and normal weight concrete, respectively.

$$\frac{k_{r1}}{k_y} = 0.6 - 0.388\ln(\mu) \tag{8}$$

$$\frac{k_{r1}}{k_y} = 0.641 - 0.479\ln(\mu) \tag{9}$$

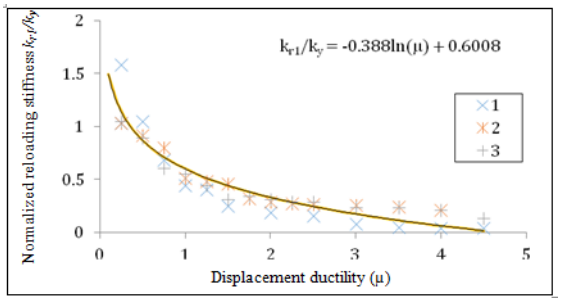

Figure 11. Variation of reloading stiffness k_{r1} with the imposed displacement ductility for lightweight concrete.

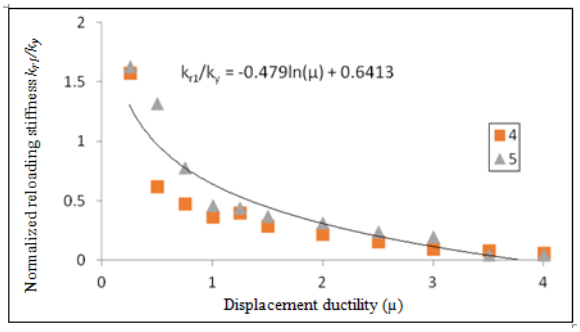

Figure 12. Variation of reloading stiffness k_{r1} with the imposed displacement ductility for normal weight concrete.

4.6 Reloading Stiffness k_{r2}

Reloading stiffness k_{r2} indicates the secant stiffness from the point of crack closure to the point of maximum load in a cycle which is shown below:

$$k_{r2}^{-} = \frac{F_i^{+} - F_{res}^{+}}{\delta_i^{+}} \tag{10}$$

Where F_i and δ_i indicate the load and the corresponding displacement in the hysteresis loop, respectively. In Figures 13 and 14, k_{r2} is shown for the lightweight and normal weight concrete, respectively. Regression analysis is done for k_{r2} based on these figures and Equations 11 and 12 are obtained respectively for the elements of lightweight and normal weight concrete, respectively:

$$\frac{k_{r2}}{k_y} = 0.862 - 0.51\ln(\mu) \tag{11}$$

$$\frac{k_{r2}}{k_y} = 0.991 - 0.48\ln(\mu) \tag{12}$$

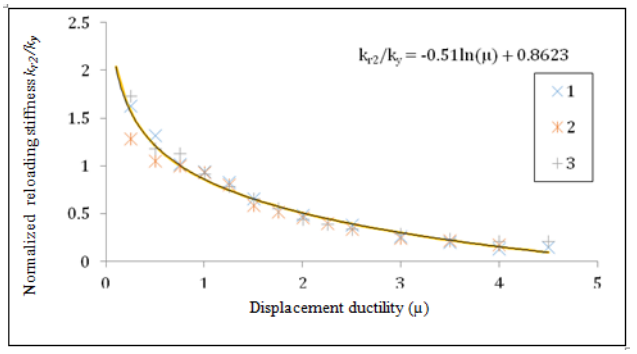

Figure 13. Variation of reloading stiffness k_{r2} with the imposed displacement ductility for lightweight concrete.

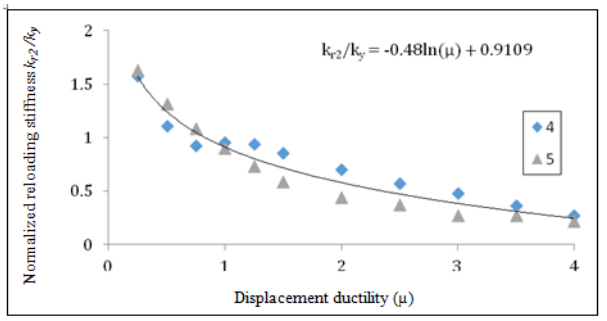

Figure 14. Variation of reloading stiffness k_{r2} with the imposed displacement ductility for normal weight concrete.

Secant stiffness degradation, unloading, and reloading based on the applied displacement ductility determine the stiffness degradation phenomenon under cyclic loading. Degradation function could be in three forms: decreasing power function, reducing exponential function, or decreasing logarithmic function. In most of the previous works, stiffness degradation caused by

repeated cycles with constant amplitude have not received great attention and earlier descriptions have not included the effect of repeating constant amplitudes of the cycles on stiffness degradation. It is obvious that, by repeating a cycle, stiffness is reduced, which is because of the reduced concrete stiffness under pressure due to repeated opening and closure of the cracks and the Bauschinger effect in the steels. In addition, an increase in the residual tensile strain increases the crack widths and reduces the bond-slip in the bar, which itself decreases the effect of tensile stiffness.

Degradation does not only depend on ductility, but also on many other parameters such as inelastic properties of materials, dissipated energy, number of cycles, loading history scenario, and duration of application. Displacement ductility used here as an effective variable for stiffness, does not include all the variables that affect the stiffness degradation and is only used to oversimplify the problem. By continuing the loading, the damage is accumulated and increased. In other words, behavior of the materials constituting the element at any time depends on the cumulative damage obtained during the past cycles and the damage increases by repeating each loading[15].

4.7 Pinching Analysis

Hysteresis loops resulted from the experimental works are not fat and are similar to Figure 15, in which tangent stiffness variations are not regular, but are affected by opening and closure of the cracks and effect of shear deformation. Therefore, in practice, the surface enclosed by a hysteresis loop is less than an ideal closed loop that is analytically obtained through nonlinear models of the materials constituting the concrete and steel. The contraction appearing in the real hysteresis loop is called pinching phenomenon.

Pinching is created due to the slip along inclined cracks. Therefore, pinching is more affected by the web cracks than by flexural cracks. Before the yielding, pinching could happen in closed hysteresis loops due to non-linearity in the concrete behavior. An ideal hysteresis curve for a symmetrical beam is presented in Figure 16. As shown in this figure, pinching can happen around the loop; however, it significantly happens in the vertical axis around the origin. According to the above descriptions, the formed contraction is only determined for the vertical axis. Contraction of the vertical axis is determined as follows:

$$x^{+} = 1 - \frac{F_{res}^{+}}{F_{id}^{+}} \qquad (13)$$

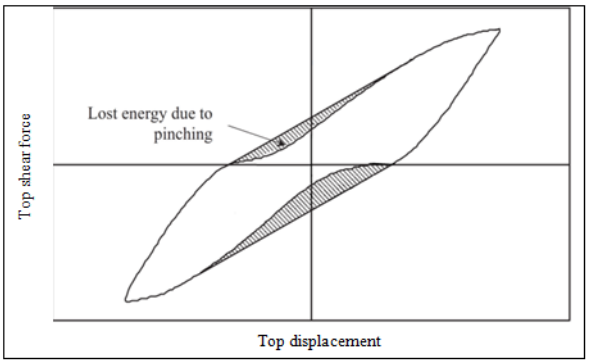

Figure 15. Typical pinched hysteretic loops in R/C elements under cyclic loading.

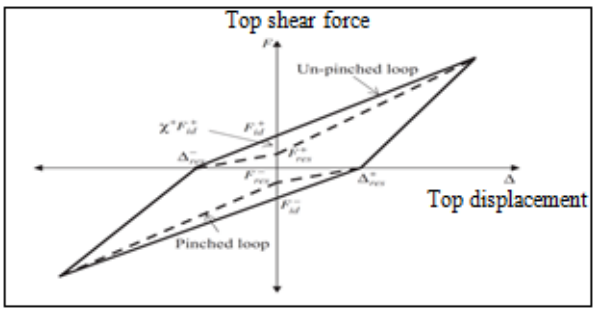

Figure 16. Schematic description of pinching index.

In the above equation, F_{id}^{+} represents the contraction in the vertical axis and x^{+}represents pinching index in the positive direction (0, x^{+}<1). A similar index has been used by Song[16]. Calculation for each direction is done separately and then the average value is determined for both directions. For this purpose, the residual strength is obtained by the test data and the ideal strength is calculated from properties of the ideal loops. The greater the pinching index, the more unfavorable the contraction would be. Pinching variations based on ductility are shown in Figures 17 and 18. Residual displacement variations are also measured for the horizontal axis based on ductility, as shown in Figures 19 and 20. By using regression, Equations 14 and 15 are obtained for the elements of lightweight and normal weight concrete, respectively.

$$\frac{\Delta_{res}}{\Delta_{y}} = 0.194\mu^{1.171} \qquad (14)$$

$$\frac{\Delta_{res}}{\Delta_{y}} = 0.248\mu^{1.562} \qquad (15)$$

In the seismic design, increase in the residual displacement increases the hysteresis energy capacity[17].

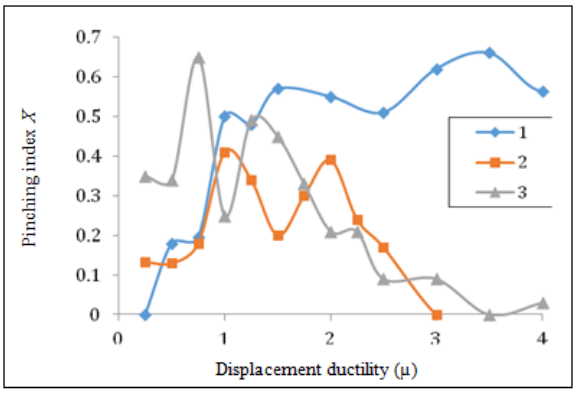

Figure 17. Pinching index–ductility relationship for lightweight concrete.

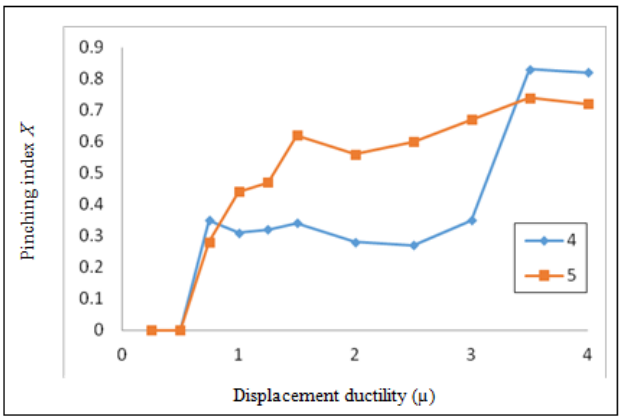

Figure 18. Pinching index–ductility relationship for normal weight concrete.

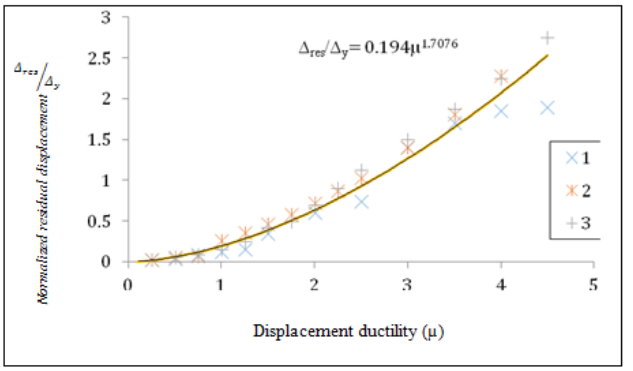

Figure 19. Residual displacement–ductility relationship for lightweight concrete.

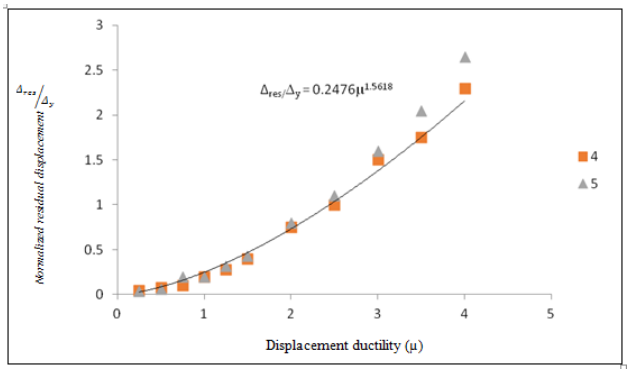

Figure 20. Residual displacement–ductility relationship for normal weight concrete.

5. Strength Degradation

Strength degradation is discussed for each specimen based on the envelopes of hysteresis loops. To provide higher accuracy for the discussion, it is necessary to identify type of failure mechanism. For all the specimens, small cracks start to grow on the tensile side of the beam at beam-column connection during the initial test steps. Increase in the tensile strain increases the crack width, which reduces the compressive strength of the concrete. These tensile strains weaken the concrete under pressure such that compressive strength of the concrete specimen becomes smaller than the compressive strength of concrete in the standard test[18]. By continuing the test and obtaining the inelastic deformation cycles, the tensile cracks do not close under the unloading and the tensile cracks on the new tensile side are connected to the tensile cracks in the previous half cycle. By continuing the test, concrete of the compressive area at the foot of the beam is gradually crushed, the longitudinal re-bar appears in this area, and the rest of the beam like a rigid element rotates around this area that resembles a concave bowl. The tests do not continue until the ultimate failure. In deformation cycles with the amplitude of 80mm, equivalent to ductility 4, no significance decrease in the strength is observed in force–deformation curve. With respect to ratio of the shear span to significant depth of the test specimens, the flexural behavior is dominant and the beams endure ductility of greater than 4. In other words, these ductile beams are controlled by deformation[8]. The most important factor that decreases the specimens' strength during the high

inelastic cycles includes re-bar cover spilt and crushing of the beam core concrete at the beam-column connection.

6. Conclusion

Flexural reinforced beams constructed of lightweight aggregate concrete with a low number of longitudinal re-bars are ductile, like the reinforced beams made of normal weight concrete, and were controlled by displacement. Also, in these beams:

- Beam stiffness, independent from strength, is reduced with increase in the displacement cycles.
- In the high deformation cycles, pinching phenomenon occurs randomly.
- Strength is not reduced with increase in amplitude of the cycles until reaching displacement ductility 4.
- Flexural behaviors of normal and reinforced lightweight aggregate concretes are the same.

7. References

1. Elwood KJ, Moehle JP. An axial capacity model for shear-damaged columns. ACI Structural Journal. 2005; 102(4):578–87.
2. Zhaoa X, Wu Y, Leung A, Fai H. Plastic hinge length in reinforced concrete flexural members. Procedia Engineering. The Proceedings of the 12th East Asia-Pacific Conference on Structural Engineering and Construction-EASEC12; 2011. p. 1266–74.
3. Chutarat N, Aboutaha RS. Cyclic response of exterior reinforced concrete beam-column joints reinforced with headed bars experimental investigation. ACI Structural Journal. 2003; 100(2):259–64.
4. Durrani AJ, Wight JK. Behavior of interior beam-to-column connections under earthquake-type loading. American Concrete Institute Journal of Proceedings. 1985; 82(3):343–9.
5. Ehsani MR, Wight JK. Exterior reinforced concrete beam-to-column connections subjected to earthquake type loading. American Concrete Institute Journal of Proceedings. 1985; 82(4):492–9.
6. Ahmad SH, Shah SP. Behavior of hoop confined concrete under high strain rates. American Concrete Institute Journal of Proceedings. 1985; 82(5):634–47.
7. Saptarshi S, Ramanjaneyulu K, Novak B, Lakshmanan N. Analytical and experimental investigations on seismic performance of exterior beam–column subassemblages of existing RC-framed building. Earthquake Eng Struct Dynam. 2013; 42(12):1785–805.
8. FEMA-273. NEHRP guidelines for the seismic rehabilitation of buildings. Washington, DC: Building Seismic Safety Council; 1997.
9. Ozcebe G, Saatcioglu M. Hysteretic shear model for reinforced concrete members. J Struct Eng. 1989; 115(1):132–48.
10. CEB. RC frames under earthquake loading: State of the art report. London: Thomas Telford; 1996. p. 316.
11. Clough RW, Johnson SB. Effects of stiffness degradation on earthquake ductility requirements. Proc 2nd Japan National Earthquake Eng Conf; Tokyo, Japan. 1966. p. 227–32.
12. Takeda T, Sozen MA, Nielsen N. Reinforced concrete response to simulated earthquakes. J Struct Div. 1970; 96(12):19–26.
13. Mander JB. Seismic design of bridge piers. UC Research Respiratory; 1983. p. 264–6.
14. Ambrisi A, Filippou FC. Modeling of cyclic shear behavior in RC members. J Struct Eng. 1999; 125(10):1143–50.
15. Rahnama M, Krawinkler H. Effects of soft soil and hysteresis model on seismic demands. The John A. Blume Earthquake Engineering Centre. 1993; 108:162–4.
16. Song JK, Pincheira JA. Spectral displacement demands of stiffness and strength degrading systems. Earthquake Spectra. 2000; 16(4):817–51.
17. Priestley M. Myths and fallacies in earthquake engineering. American Concrete Institute; 1997. p. 231–54.
18. Vecchio FJ, Collins MP. Modified compression-field theory for reinforced concrete elements subjected to shear. Journal of the American Concrete Institute. 1986; 83(2):219–31.